Lecture 4 – Results Analysis & Beyond Docking

Goal

The goal of this lecture is to teach how to critically analyze docking results, interpret scores, evaluate binding poses, and extend docking studies using advanced techniques. Docking generates predictions of ligand-receptor interactions, but these predictions are approximations. Understanding their limitations and validating results against experimental data are essential for meaningful conclusions in drug discovery.

Understanding Good Results

Not all docking outputs are equally informative. To distinguish reliable predictions, it is important to look beyond raw docking scores. Some strategies are listed below.

Pose clustering

When multiple runs produce similar ligand conformations, these clusters suggest that the ligand has a preferred binding mode and the sampling algorithm is capturing a realistic energy minimum. Conversely, widely scattered poses indicate uncertainty or insufficient sampling.

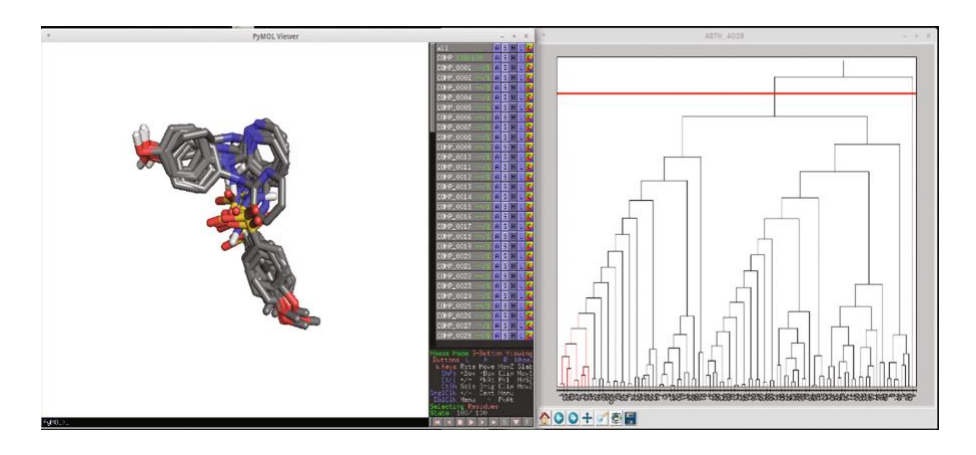


Figure 1: Example of visualization of results from AutoDock, clustered hierarchically¹.

Example 1: For kinase inhibitors docking to CDK2, a rigid receptor often produces scattered poses with no clear cluster. Only when sampling multiple conformations of the activation loop do clusters emerge, reflecting realistic binding orientations².

Score funnels

These plots show docking score as a function of pose deviation (e.g., RMSD from a reference structure). Ideally, the lowest-energy poses cluster near the expected binding mode, forming a funnel-like distribution. A clear funnel indicates that the scoring function can discriminate between

realistic and unrealistic poses. Flat or noisy distributions suggest that the scoring function may lack selectivity, and low-energy poses might be artifacts.

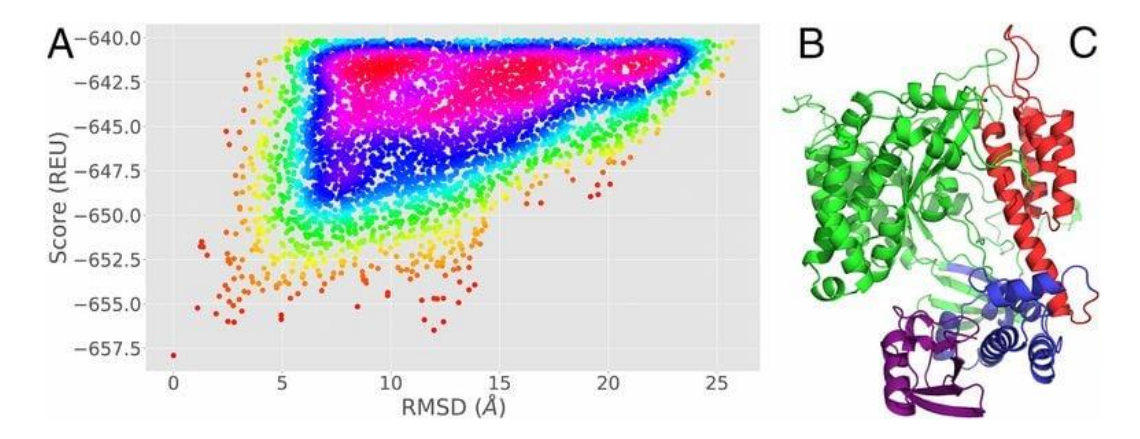


Figure 2: Modeling of the interaction between ExoU, a toxin secreted by psueomonas aureginosa, and monoubiquitin. (A) A scoring funnel plot showing Rosetta energy score (REU) versus RMSD for the top 5,000 models. The funnel's trend is indicative of convergence toward a low-energy binding mode. (B) Best-scoring complex with ExoU catalytic (green), bridging (blue), and membrane localization (red) domains in complex with ubiquitin (purple)³.

Example 1: Docking flexible ligands without accounting for receptor side-chain flexibility can yield a flat score—RMSD plot, where low-energy poses are spread widely and the scoring function fails to discriminate the correct binding mode.

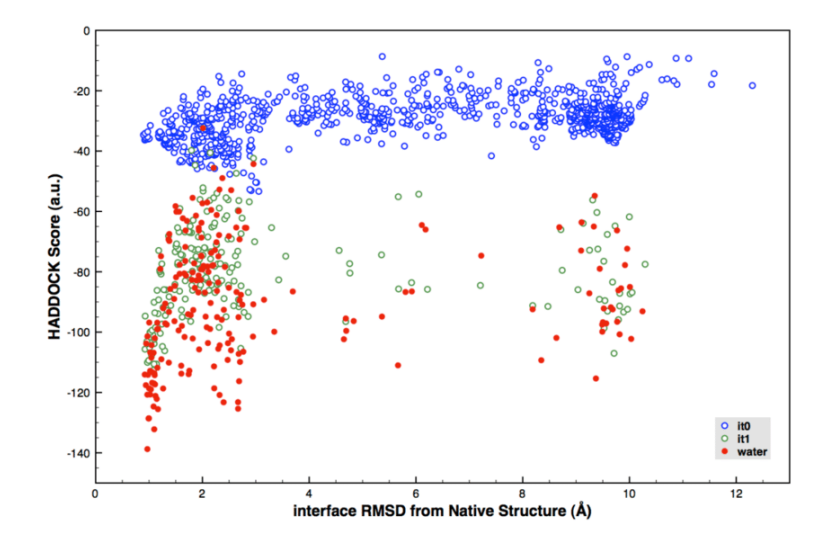


Figure 3: Plot of HADDOCK scores vs. interface RMSD from the reference complex (PDB:1GGR) for the three stages of the docking protocol (blue, green, and red, for it0, it1, and water refinement respectively). One can clearly see a funnel at low RMSD values when water refinement is being considered. In it0 and it1, the RMSD vs. HADDOCK score is flat, indicating no convergence and the scoring function cannot reliably identify the correct binding mode⁴.

Chemically plausible interactions

Docking scores alone cannot guarantee correct hydrogen bonds, salt bridges, or hydrophobic contacts. Even low-energy poses must be examined visually for steric clashes and realistic complementarity with the receptor.

Example 1: Docking HIV-1 protease inhibitors may yield a low-energy pose where the ligand avoids the catalytic Asp25/Asp25' residues. Despite the favorable score, this pose is biologically irrelevant because the essential hydrogen bonds are missing⁵.

Example 2: In docking BACE1 inhibitors, a ligand might occupy the flap region in an unrealistic conformation, sterically clashing with conserved flap residues. Even with a low docking score, such a pose would be dismissed upon visual inspection⁶.

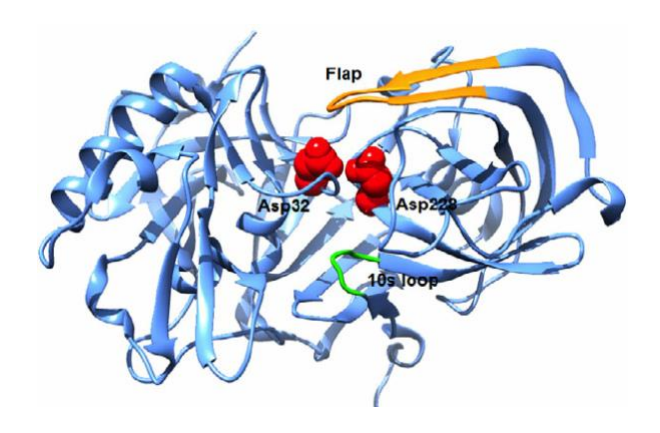


Figure 4: Crystal structures of isolated BACE1, highlighting the active site aspartate residues: Asp32 and Asp228 (red spacefill representation), hairpin loop termed 'flap' (orange) and the 10s loop (green)⁷.

Evaluating Docking Results

Docking scores provide a **relative ranking**, not absolute binding free energies. Many users mistakenly interpret docking scores as experimental ΔG , but scoring functions are simplifications that ignore entropic contributions, solvation, and protein flexibility. For example, in docking multiple inhibitors to EGFR, some weak binders may receive more favorable scores than strong ones because the scoring function overestimates hydrophobic contacts or neglects desolvation penalties.

RMSD analysis

This is helpful when a reference ligand structure is available. An RMSD under 2 Å generally indicates a successful prediction, but this metric has limitations. Minor deviations in side-chain positions may increase RMSD without invalidating a pose, and multiple poses can have similar RMSDs but different key interactions. RMSD should therefore be considered alongside visual inspection and chemical reasoning.

Example 1 (hypothetical): Redocking ATP to CDK2 produces a predicted pose with an RMSD of 1.2 Å relative to the crystal structure. This is considered successful, even though a nearby lysine side chain shifts slightly to accommodate the ligand. The small side-chain deviation increases RMSD slightly but does not invalidate the binding mode.

Example 2 (hypothetical): In docking imatinib to BCR-ABL, two predicted poses both have RMSDs around 1.8 Å, but one correctly forms the key hydrogen bond with the hinge region while the other does not. This shows that similar RMSD values can mask important differences in interactions, highlighting the need for visual inspection.

Library ranking

Virtual screening campaigns rank thousands of ligands, but top-scoring compounds are not guaranteed actives. Artifacts and scoring biases are common. Therefore, ranking should be combined with pose inspection, clustering, and comparison with experimental SAR data. Integrating multiple evaluation criteria increases confidence in selecting promising candidates.

Example 1 (hypothetical): In a virtual screen of 50,000 compounds against EGFR, the top-scoring ligand according to the docking program fails to inhibit kinase activity in vitro, while a ligand ranked 15th shows strong inhibition. The scoring function overestimated the contribution of hydrophobic contacts in the top-ranked compound.

Example 2 (hypothetical): Docking 10,000 inhibitors to HIV-1 protease shows that several low-scoring compounds adopt poses that clash sterically with the flaps. Despite favorable scores, these compounds are false positives. Cross-checking with clustering and visual inspection allowed identification of truly promising candidates.

Visual Inspection

Visual inspection remains critical despite advances in scoring functions. Docking software cannot always capture subtle chemical interactions, and some top-scoring poses may be unrealistic. Analysts should examine:

- Hydrogen bonds, salt bridges, and hydrophobic contacts
- Steric clashes and strained conformations
- Consistency with known SAR or mutagenesis data

This process helps identify "good scores but bad poses." For example, a ligand might occupy a pocket region in a way that requires extreme side-chain movement, which is chemically implausible. Visual inspection ensures that top-ranked compounds are truly reasonable candidates for further study.

Validation Strategies

Validation builds confidence in docking predictions.

Self-docking (redocking) tests whether the protocol can reproduce a known ligand pose. If the predicted pose matches the crystal structure, the docking setup is likely valid.

Cross-docking involves docking ligands into multiple receptor conformations. This is useful for flexible proteins such as kinases or GPCRs, where induced fit can alter the binding site. Cross-docking evaluates the robustness of the docking protocol across different protein states.

Example 1: Docking dasatinib into three different BCR-ABL conformation: active, intermediate inactive, and inactive, shows that dasatinib binds selectively to the active (open) conformation⁸.

Integration with experimental data provides additional validation. If a docking pose predicts a hydrogen bond with a key residue, mutating that residue should reduce binding experimentally. Combining computational predictions with mutagenesis, SAR, or biochemical assays strengthens confidence in the results.

Advanced Docking Approaches

Standard rigid docking has limitations, which advanced techniques address:

Induced fit docking

This allows receptor side chains or backbone segments to move in response to ligand binding, accommodating flexible pockets such as kinase activation loops or GPCR binding sites.

Hsp90 inhibitors

Hsp90 is a molecular chaperone with a highly flexible N-terminal ATP-binding pocket. When inhibitors like geldanamycin are docked using rigid receptor models, the predicted poses often fail to reproduce crystallographic interactions because the lid domain of Hsp90 shifts to accommodate the ligand. Induced fit docking allows side chains and portions of the backbone to move, capturing these conformational changes⁹. This approach reproduces the correct hydrogen bonds between the inhibitor and key residues such as Asp93 and Lys58, and accurately positions hydrophobic moieties in the pocket. By accounting for receptor flexibility, induced fit docking improves both pose accuracy and ranking of potential inhibitors in Hsp90 drug discovery campaigns.

Covalent docking

This models ligands that form chemical bonds with the receptor, accounting for geometric constraints and energetic penalties. Covalent inhibitors, such as cysteine-targeting kinase inhibitors, require specialized scoring and sampling.

Ras G12C inhibitors

KRAS G12C mutants are oncogenic drivers in certain cancers. Covalent inhibitors, such as sotorasib, target the cysteine at position 12 in the switch-II pocket. Standard docking cannot model bond formation, so covalent docking is used to account for both the reaction geometry and

energetic penalties of forming the covalent bond. Covalent docking can predict proper electrophile orientation and optimize noncovalent interactions¹¹. This allows identification of potent compounds that specifically react with the mutant cysteine while minimizing off-target effects.

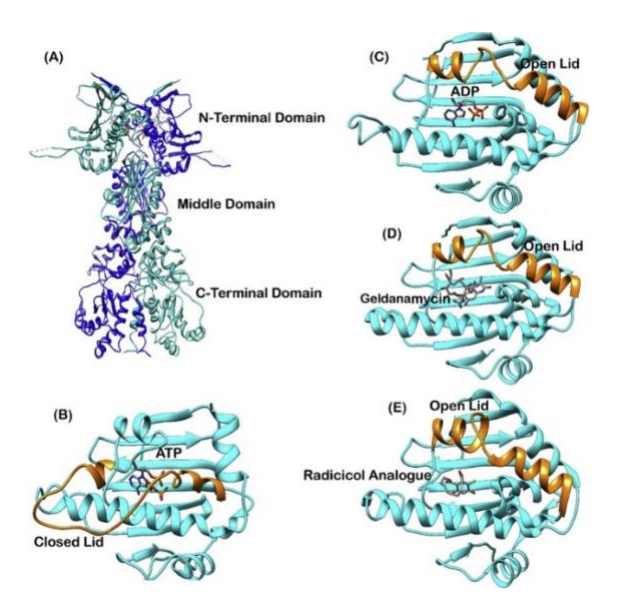


Figure 5: (A) Structure of Hsp90, (B) Closed lid conformation of ATP binding pocket in Hsp90-ATP complex, (C), (D) and (E) showing closed lid conformation of ATP binding pocket in Hsp90-ADP, Hsp90-geldelamycin and Hsp90-radicicol analogue complex respectively¹⁰.

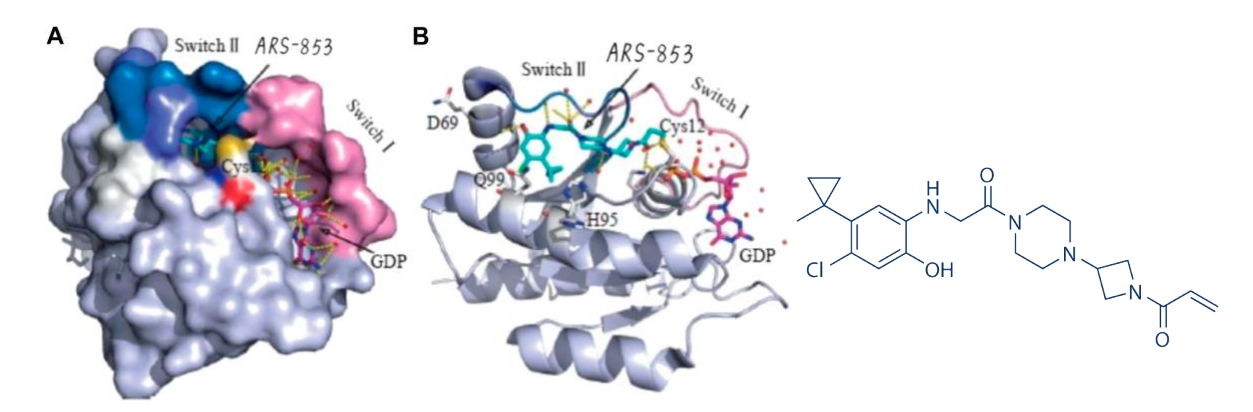


Figure 6: (A) and (B): Representation of KRAS G12C in complex with ARS-853. The acrylamide of ARS-853 can form covalent bond with 12 cysteine and extend to switch II region. (C) Structure of ARS-853¹².

Macrocycle and Peptide Docking

Cyclosporine and cyclophilin A

Cyclosporine A (CsA) is a cyclic undecapeptide immunosuppressant that binds tightly and stereospecifically to cyclophilin A (CypA), with binding strongly dependent on the macrocycle's conformational state. Standard docking methods often struggle with such ligands because they

inadequately sample the vast torsional space and ring conformations of macrocycles. To address this, ensemble and macrocycle-specific docking approaches have been developed that systematically explore multiple conformers, improving the ability to reproduce crystallographic poses. In the case of cyclophilin A, docking studies using cyclosporine A have demonstrated that incorporating receptor flexibility improves the recovery of accurate binding poses consistent with crystallographic data¹³. These findings underscore that specialized approaches for macrocycle docking are essential for modeling complex ligands like cyclosporine and can guide the design of new analogs with improved potency and pharmacokinetic properties.

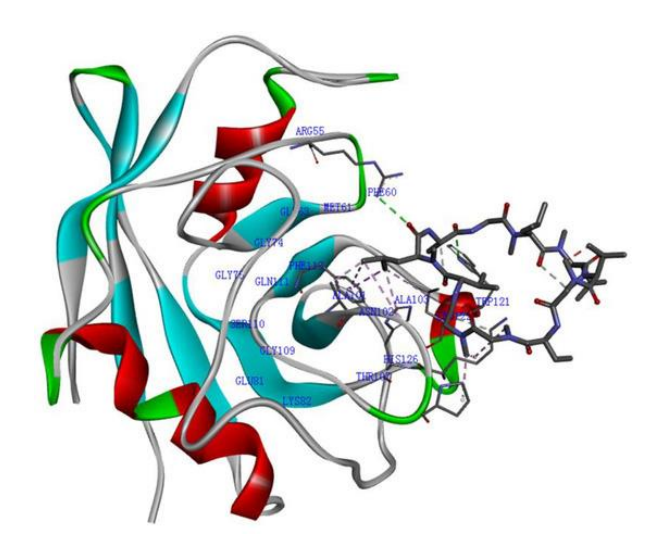


Figure 7: The cyclophilin A–CsA complex. Cyclophilin A binding site (PDB:1CWA). β-sheets in light blue, α-helices in red in cyclophilin A structure. CsA is indicated in black and gray. The 19 residues of cyclophilin A bind in CsA are dark blue¹⁴.

High-Throughput Virtual Screening (HTVS)

This approach leverages GPUs and hierarchical docking to handle millions of compounds efficiently. Post-docking analysis—clustering, visual inspection, and experimental cross-validation—remains essential to avoid false positives.

SARS-CoV-2 PLpro inhibitors

During the COVID-19 pandemic, millions of compounds were screened virtually against targets from SARS-CoV-2 using GPU-accelerated docking. HTVS efficiently handled the large dataset, and post-docking analysis using clustering and visual inspection prioritized compounds with plausible binding poses¹⁵. Subsequent biochemical testing validated several hits, demonstrating that HTVS combined with careful pose evaluation can rapidly identify promising antiviral candidates.

References

(1) Varela-Salinas, G.; García-Pérez, C. A.; Peláez, R.; Rodríguez, A. J. Visual Clustering Approach for Docking Results from Vina and Autodock. In *Lecture Notes in Computer*

- Science (including subseries Lecture Notes in Artificial Intelligence and Lecture Notes in Bioinformatics); 2017; Vol. 10334 LNCS. https://doi.org/10.1007/978-3-319-59650-1 29.
- (2) Duca, J. S.; Madison, V. S.; Voigt, J. H. Cross-Docking of Inhibitors into CDK2 Structures. 1. *J Chem Inf Model* 2008, *48* (3). https://doi.org/10.1021/ci7004274.
- (3) Tessmer, M. H.; Anderson, D. M.; Pickrum, A. M.; Riegert, M. O.; Moretti, R.; Meiler, J.; Feix, J. B.; Frank, D. W. Identification of a Ubiquitin-Binding Interface Using Rosetta and DEER. *Proc Natl Acad Sci U S A* 2018, *115* (3). https://doi.org/10.1073/pnas.1716861115.
- (4) Rodrigues, J. P. G. L. M.; Karaca, E.; Bonvin, A. M. J. J. Information-Driven Structural Modelling of Protein–Protein Interactions. *Methods in Molecular Biology* 2015, *1215*. https://doi.org/10.1007/978-1-4939-1465-4 18.
- (5) Razzaghi-Asl, N.; Sepehri, S.; Ebadi, A.; Miri, R.; Shahabipoura, S. Effect of Biomolecular Conformation on Docking Simulation: A Case Study on a Potent HIV-1 Protease Inhibitor. *Iranian Journal of Pharmaceutical Research* 2015, *14* (3).
- (6) Bajda, M.; Jończyk, J.; Malawska, B.; Filipek, S. Application of Computational Methods for the Design of BACE-1 Inhibitors: Validation of in Silico Modelling. *Int J Mol Sci* 2014, *15* (3). https://doi.org/10.3390/ijms15035128.
- (7) Kumalo, H. M.; Bhakat, S.; Soliman, M. E. Investigation of Flap Flexibility of β-Secretase Using Molecular Dynamic Simulations. *J Biomol Struct Dyn* 2016, 34 (5). https://doi.org/10.1080/07391102.2015.1064831.
- (8) Laurini, E.; Posocco, P.; Fermeglia, M.; Gibbons, D. L.; Quintás-Cardama, A.; Pricl, S. Through the Open Door: Preferential Binding of Dasatinib Tothe Active Form of BCR-ABL Unveiled by in Silico Experiments. *Mol Oncol* 2013, 7 (5). https://doi.org/10.1016/j.molonc.2013.06.001.
- (9) Lauria, A.; Ippolito, M.; Almerico, A. M. Inside the Hsp90 Inhibitors Binding Mode through Induced Fit Docking. *J Mol Graph Model* 2009, 27 (6). https://doi.org/10.1016/j.jmgm.2008.11.004.
- (10) Verma, S.; Goyal, S.; Jamal, S.; Singh, A.; Grover, A. Hsp90: Friends, Clients and Natural Foes. *Biochimie*. 2016. https://doi.org/10.1016/j.biochi.2016.05.018.
- (11) Zhu, K.; Li, C.; Wu, K. Y.; Mohr, C.; Li, X.; Lanman, B. Modeling Receptor Flexibility in the Structure-Based Design of KRASG12C Inhibitors. *J Comput Aided Mol Des* 2022, *36* (8). https://doi.org/10.1007/s10822-022-00467-0.
- (12) Yang, A.; Li, M.; Fang, M. The Research Progress of Direct KRAS G12C Mutation Inhibitors. *Pathology and Oncology Research*. 2021. https://doi.org/10.3389/pore.2021.631095.
- (13) Akten, E. D.; Cansu, S.; Doruker, P. A Docking Study Using Atomistic Conformers Generated via Elastic Network Model for Cyclosporin a/Cyclophilin a Complex. *J Biomol Struct Dyn* 2009, 27 (1). https://doi.org/10.1080/07391102.2009.10507292.
- (14) Zhao, X.; Zhao, X.; Di, W.; Wang, C. Inhibitors of Cyclophilin A: Current and Anticipated Pharmaceutical Agents for Inflammatory Diseases and Cancers. *Molecules*. 2024. https://doi.org/10.3390/molecules29061235.
- (15) Rogers, D. M.; Agarwal, R.; Vermaas, J. V.; Smith, M. D.; Rajeshwar, R. T.; Cooper, C.; Sedova, A.; Boehm, S.; Baker, M.; Glaser, J.; Smith, J. C. SARS-CoV2 Billion-Compound Docking. *Sci Data* 2023, *10* (1). https://doi.org/10.1038/s41597-023-01984-9.